

Atomic coherence effects in few-cycle pulse induced ionization

Viktor Ayadi^{1,*}, Mihály G. Benedict², Péter Dombi^{1,3}, and Péter Földi^{2,3}

¹MTA "Lendület" Ultrafast Nanooptics Group, Wigner Research Centre for Physics, Konkoly-Thege M. út 29-33, H-1121 Budapest, Hungary

²Department of Theoretical Physics, University of Szeged, Tisza Lajos körút 84, H-6720 Szeged, Hungary

³ELI-ALPS, ELI-HU Non-profit Ltd., Dugonics tér 13, H-6720 Szeged, Hungary

*ayadi.viktor@wigner.mta.hu

ABSTRACT

The interaction of a short, few-cycle light pulse and an atom which is prepared initially in a superposition of two stationary states is shown to exhibit strong signatures of atomic coherence. For a given waveform of the laser pulse, appropriate quantum mechanical relative phase between the constituents of the initial superposition can increase the ionization probability by a factor of three. A similarly strong effect can be observed when the waveform of the ionizing pulse is changed. These results allow for intuitive explanations, which are in agreement with the numerical integration of the time dependent Schrödinger equation.

Introduction

During the process of photoionization induced by few-cycle, near infrared laser pulses, both the period of the external field oscillations and the duration of the complete pulse are on the same timescale as the internal atomic dynamics. This suggests that the details of the electron emission are determined by the waveform of the exciting laser pulse, in other words, besides the temporal envelope of the pulse, the carrier-envelope phase (CEP)^{1,2} also plays an important role in the process. Similar CEP-dependent effects were shown to appear in various laser-induced processes including high harmonic generation³⁻⁵, above-threshold ionization (ATI)^{6,7}, non-sequential double ionization⁸ and multi-photon induced photoemission^{9,10}.

Recently, the excitation and ionization probabilities from ground state atomic hydrogen have been studied in intense short pulses¹¹ by numerically integrating the time dependent Schrödinger equation (TDSE). The interesting features found in that paper are related to the ratio of the ionization and excitation probabilities as a function of the intensity of the incoming laser field. As it was found, whenever an ATI peak merges into the continuum as a consequence of the increasing ponderomotive force, the ionization yield has a minimum, while the excitation probability increases. Let us note that phase relations play an important role in ATI. This was pointed out in¹², where the influence of a chirp in the excitation pulse was investigated, as well as in¹³, where the effect of a sudden phase jump during the excitation was considered.

In the current paper we also consider short pulse induced ionization processes, but – in contrast to previous studies – we focus on the interplay between the internal atomic dynamics and that induced by the intense laser field. To this end we consider initial states that are superpositions of dipole coupled stationary bound states. There is a great variety of important effects in atom-field interactions, where atomic coherence between atomic levels play a role. Coherent population trapping, electromagnetically induced transparency and lasing without inversion, are the most significant ones in the normal intensity regime. For an overview of all these effects see¹⁴. Coherent superpositions as initial states in the context of high harmonic generation (HHG) have been investigated in Refs.¹⁵⁻¹⁷. Atomic coherence plays also a decisive role in strong field atomic stabilization, predicted first in^{18,19}, see also^{20,21}. In order to observe this effect, however, pulses of duration of hundreds of femtoseconds are necessary.

It is natural to expect that atomic coherence may influence the transitions to a third energy level also in the field of an intense, few-cycle pulse, when the third level falls in the continuum. We choose the initial conditions as coherent superpositions of stationary atomic states in order to explore the details of this process. The atom and the field are coupled through the dipole interaction, and the expectation value of the dipole moment operator in these initial states is generally non-zero, it oscillates with the appropriate Bohr frequency. When the frequency of these ("internal, atomic") oscillations is comparable with that of the laser field, the essence of the pronounced CEP-dependence of the problem can be understood using a simple, classical picture: The relative phase of the internal oscillations and that of the external excitation determines whether they interfere constructively or destructively. When the "swing" of the internal dipole oscillations is excited in an appropriate phase, the amplitude increases and the ionization yield has a maximum. On the other hand, when the external field has to "work against"

the internal oscillations, the ionization probability is considerably lower. Additionally, when the frequency of the two types of oscillations are not close enough, this effect becomes weaker. Here, we will show that our fully quantum mechanical treatment is qualitatively in accordance with the intuitive picture described above.

Clearly, it is not only the atomic coherence that determines the ionization probability: as one can expect, the energy of the initial states is the most important parameter. As we shall see, the ionization yield is not increasing monotonically with the expectation value of the energy in the initial state, which can be understood by inspecting the distance of the first ATI peak from the limit of the continuum. These effects define the ionization probability on which oscillations caused by atomic coherence phenomena are superimposed.

Technically, we solve the time dependent Schrödinger equation of a hydrogen-like atom in an intense, pulsed, few-cycle, near infrared laser field. Our approach is based on the numerical methods that were used e.g., in Refs. [22,23](#). We use realistic parameters for the high-power ultrashort laser pulses with durations as short as a few optical cycles that have already been available as research tools^{[24-26](#)}. The results show strong CEP-dependence of the ionization signal for initial superpositions of s and p states with different principal quantum numbers. Additionally, we study how the relative phase between the components of these superpositions influences the dynamics of the atomic dipole moment and the ionization process. We show that the CEP dependence of the ionization process can be detectable for pulse durations up to 22 fs (8 optical cycles), which is remarkably long in this context. Note that if the preparation of the initial superpositions is assumed to be achieved by a conventional, many cycle pulse of appropriate area^{[27](#)}, the relative phase of the s and p components is proportional to the delay between the preparation and the few-cycle pulses. As we discuss in the second and the fourth sections, the time scales of spontaneous emission, as well as that of the “conventional,” low intensity, many cycle excitation compared with the ultrashort ionization allows a convenient way of preparing the initial superpositions.

The current paper is organized as follows. In the second section we introduce the specific initial states we consider, describe the excitation pulse with a carrier-envelope phase, as well as the method of integrating the TDSE. Next we present and discuss our results, and analyse the possible experimental realization. The conclusions can be found in the final section.

Model

In order to focus on the interplay between the internal, atomic dynamics and that of induced by the strong laser pulse, we consider three types of initial superpositions of hydrogenic states

$$\psi_{23}(c, \delta) = c_{2s}\phi_{2s} + c_{3p}\exp(i\delta)\phi_{3p}, \quad (1)$$

$$\psi_{34}(c, \delta) = c_{3s}\phi_{3s} + c_{4p}\exp(i\delta)\phi_{4p}, \quad (2)$$

$$\psi_{45}(c, \delta) = c_{4s}\phi_{4s} + c_{5p}\exp(i\delta)\phi_{5p}, \quad (3)$$

where $\phi_{n\ell}$ are normalized nonrelativistic hydrogenic eigenstates with magnetic quantum number $m = 0$. The coefficients $c_{n\ell}$ denote the real amplitudes of the corresponding components in the superpositions, while δ is the relative phase between them. Note that for the realistic laser parameters we use [see after Eq. [5](#)], superpositions of the $1s$ and $2p$ states lead to negligible ionization probability.

The time dependence of the nonstationary states ([1 - 3](#)) are determined by the difference between the energy eigenvalues, i.e., the Bohr frequencies $\omega_{nn'} = \omega_n - \omega_{n'} = 20,671 \left(\frac{1}{n'^2} - \frac{1}{n^2} \right) (\text{fs})^{-1}$ as:

$$\psi_{nn'}(c, \delta, t) = e^{-i\omega_{nn'}t} \{ c_{ns}\phi_{ns} + c_{n'p}\exp[i(\delta + \omega_{nn'}t)]\phi_{n'p} \}, \quad (4)$$

where the global phase factor has no physical consequences. We assume that this is the wavefunction of the state until the strong external driving is switched on. The initial superpositions $\psi_{nn'}(c, \delta, t = 0)$ can be realized by using resonant, many cycle preparation pulses of low intensity, where the pulse area (that is proportional to the time integral of the electric field amplitude) determines the magnitude of the coefficients c ^{[27](#)}. E.g., the state ψ_{23} can be achieved by an ultraviolet excitation of the $1s$ - $3p$ Lyman beta transition followed by a laser pulse of appropriate area at the wavelength of the Balmer alpha line in the visible. Another possibility is to start the coherent superposition from the lower, metastable $2s$ state, which can be achieved by various techniques, as described in^{[28](#)}. Note that the duration of the preparation process is still considerably shorter than the lifetime of the states ([1 - 3](#))^{[29](#)}. For more details see the fourth section. As it is suggested by the second term in Eq. (4), the relative phase δ in Eqs. ([1 - 3](#)) can be controlled by changing the delay between the preparation pulse and the few-cycle one.

Our main purpose is to investigate how short, intense, few-cycle laser pulses modify the free time evolution given by Eq. (4) – in a parameter range where the duration of the external disturbance is comparable with the time scale of the Bohr oscillations. The electric field of the few-cycle laser pulse is assumed to be polarized in the z direction, and its time dependence is written as

$$E(t) = E_0 \sin^2(\pi t/\tau) \cos(\omega t + \varphi_{\text{CEP}}), \quad (5)$$

where the envelope function (\sin^2) is assumed to be zero when $t < 0$ or $t > \tau$ ³⁰, and ω is the angular frequency corresponding to a central wavelength of 800 nm. Additionally, unless stated otherwise, we use $\tau = 12$ fs [corresponding to 4.4 fs intensity full width at half maximum (FWHM)] and $E_0 = 2.5$ GV/m peak field strength. These parameters are experimentally achievable using current Ti:sapphire technology^{25,26,31}, and they induce comparable ionization probabilities from the initial states (1 - 3).

We use atomic units and solve the time dependent Schrödinger equation (TDSE) numerically in the coordinate representation:

$$i \frac{\partial}{\partial t} \psi(\mathbf{r}, t) = H(t) \psi(\mathbf{r}, t), \quad (6)$$

where the Hamiltonian takes the form

$$H(\mathbf{r}, t) = H_0(\mathbf{r}) + H_1(\mathbf{r}, t) = \left[-\frac{\Delta}{2} - \frac{1}{r} \right] + E(t)z. \quad (7)$$

Note that the position vector $\mathbf{r} = (x, y, z)$ corresponds to the relative (electron-nucleus) coordinates, i.e., we are working in the center of mass frame. The light-atom interaction described by $H_1 = E(t)z$ is written using the dipole approximation (which can be shown to be valid in the parameter range considered here^{32,33}).

Note that various numerical methods can be used for the solution of the TDSE as a partial differential equation, for example: the method of lines, split step Fourier, etc. For our purposes, the most efficient approach was found to be based on spherical harmonics expansion²². That is, we use spherical coordinates and write ψ as

$$\psi(r, \theta, t) = \sum_{\ell=0}^{\ell_{\max}} \frac{\Phi_{\ell}(r, t)}{r} Y_{\ell}^0(\theta), \quad (8)$$

where, due to the cylindrical symmetry, no summation with respect to m appears: we can restrict our calculations to $m = 0$. (In other words, there is no ϕ dependence.) Note that Eq. (8) means a separation of the $1/r$ dependence of the wave function, resulting in the following equations for $\Phi_{\ell}(r, t)$ and $\hat{\psi} = r\psi$:

$$\hat{H}_0 \Phi_{\ell}(r, t) = \left[-\frac{1}{2} \left(\frac{\partial^2}{\partial r^2} - \frac{\ell(\ell+1)}{r^2} \right) - \frac{1}{r} \right] \Phi_{\ell}(r, t), \quad (9)$$

$$i \frac{\partial}{\partial t} \hat{\psi}(\mathbf{r}, t) = [\hat{H}_0 + \hat{H}_1(t)] \hat{\psi}(\mathbf{r}, t). \quad (10)$$

Since H_1 does not contain derivatives with respect to \mathbf{r} , the interaction $\hat{H}_1 = H_1$ contains only the z coordinate, the nonzero matrix elements of which are well known, and read

$$\langle Y_{\ell}^0 | \cos \theta | Y_{\ell+1}^0 \rangle = \frac{\ell+1}{\sqrt{(2\ell+1)(2\ell+3)}}. \quad (11)$$

The radial equation above is discretized by a special finite difference (FD) scheme, which was presented in details in Ref.²³ and relies on the alternating direction implicit (ADI) method³⁴.

For our calculations ℓ_{\max} was chosen to be 100 and the radial grid consisted of 6000 points. The size of the computational grid we have used was 600 atomic units (≈ 31.7 nm) in both directions. These numbers were found to be sufficient: The populations of the states close to the maximal ℓ and r values were always negligible in our calculations, i.e., there were no numerical artifacts do to "reflections" at the edges of the grid.

The discretization of Eq. (10) allows the numerical determination of the eigenvectors $|\Psi_n\rangle$ and eigenvalues ε_n of H_0 . The analytically known bound part of the spectrum [states with negative energies, like ϕ_{ns} and ϕ_{np} in Eqs. (1 - 3)] were appropriately reproduced in this way. States with positive values of ε_n correspond to the continuous part of the spectrum. Using a projector

$$\Pi_i = \sum_{n, \varepsilon_n > 0} |\Psi_n\rangle \langle \Psi_n| \quad (12)$$

on these states, the ionization probability can be defined as:

$$P_i(t) = \|\Pi_i \psi(\mathbf{r}, t)\|^2 = \sum_{n, \varepsilon_n > 0} |\langle \Psi_n | \psi(\mathbf{r}, t) \rangle|^2. \quad (13)$$

Note that since the complete state is normalized in the sense above ($\sum_n |\langle \Psi_n | \psi(\mathbf{r}, t) \rangle|^2 = 1$, within numerical precision), P_i defined in Eq. (13) has indeed a clear probabilistic interpretation, and after the pulse (i.e., for $t > \tau$), P_i can be determined experimentally.

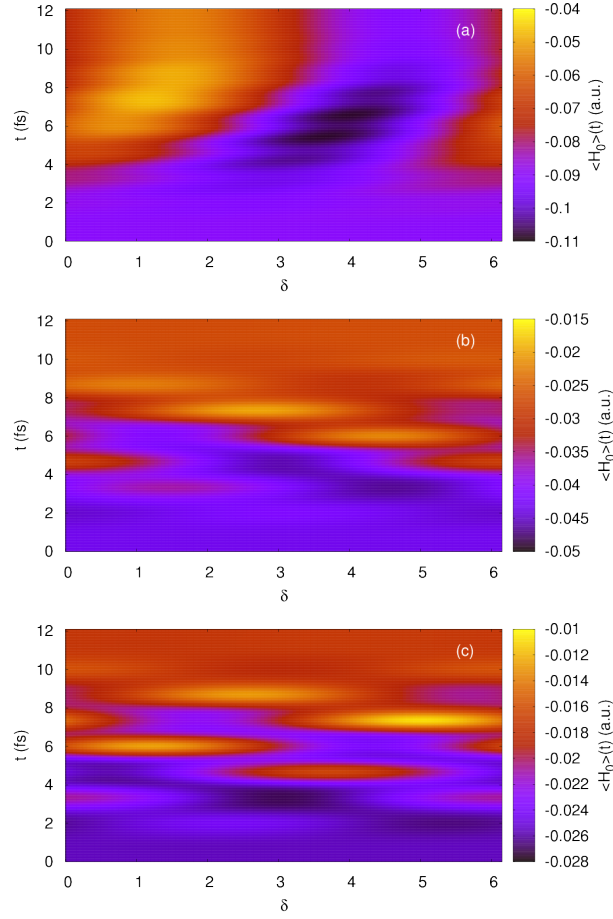


Figure 1. The time and the initial phase (δ) dependence of $\langle H_0 \rangle(t)$ for the initial states: (a) ψ_{23} , (b) ψ_{34} , (c) ψ_{45} , with $c_{ns} = c_{n+1p} = 1/\sqrt{2}$ for all cases. The CEP of the laser pulse was chosen to be 0 for all three states. Additional parameters: 800nm central wavelength, $\tau = 12$ fs and $E_0 = 2.5$ GV/m.

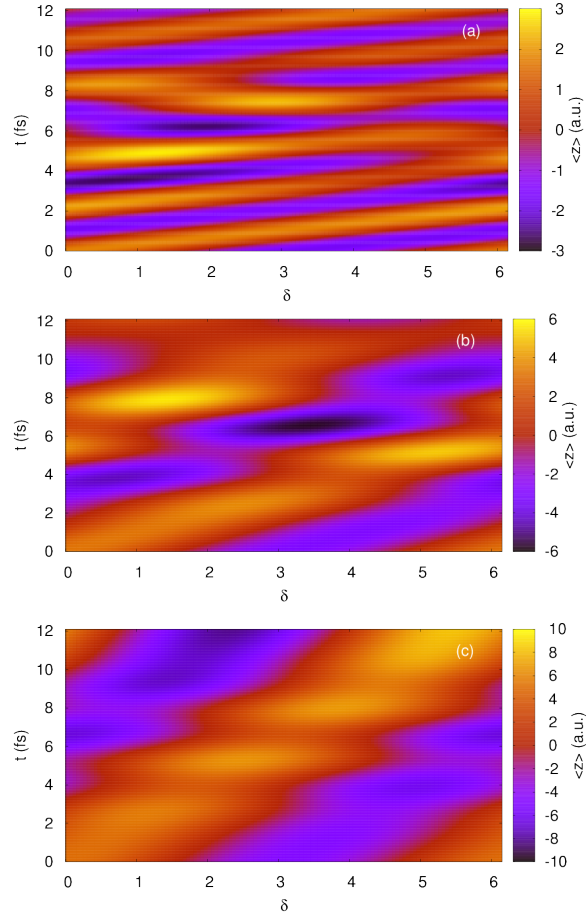


Figure 2. The time and the initial phase (δ) dependence of $\langle z \rangle$ for the initial states: (a) ψ_{23} , (b) ψ_{34} , (c) ψ_{45} (equal weight superpositions, $c_{ns} = c_{n+1p} = 1/\sqrt{2}$). The parameters of the exciting pulse are the same as in Fig. 1

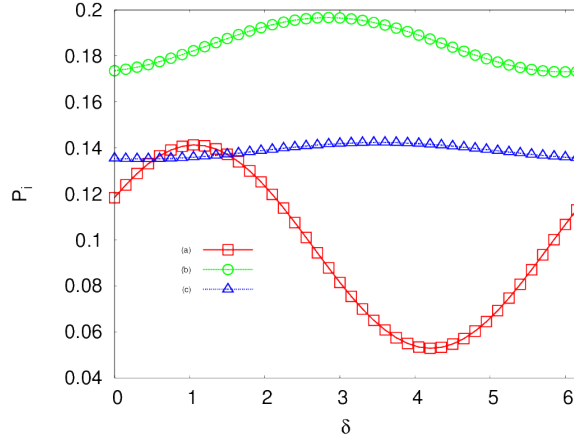


Figure 3. The phase (δ) dependence of the final ionization probabilities for the initial states: (a) ψ_{23} , (b) ψ_{34} , (c) ψ_{45} (equal weight superpositions). The CEP of the laser pulse was chosen to be 0 for all three states. The parameters of the exciting pulse are the same as in Fig. 1.

Results and discussion

The role of the atomic coherence

First we concentrate on superpositions with equal weights of the constituents [i.e., all the coefficients c are equal to $1/\sqrt{2}$ in Eqs. (1 - 3)] and investigate the dependence of the ionization process on the relative phase δ . During the solution of the TDSE, we calculated the expectation value $\langle z \rangle$, which is proportional to the z component of the dipole moment (all other components of which are constant zero as a consequence of the cylindrical symmetry). Although our system is not closed, and consequently energy is not conserved, $\langle H_0 \rangle(t)$ provides information related e.g., to the population of the energy levels. The ionization probability P_i measures the population of energy levels with positive energy.

Now, let us focus on Figs. 1-3, where $\phi_{\text{CEP}} = 0$ is fixed and we only varied δ . Fig. 1 shows $\langle H_0 \rangle$, for the three different initial superpositions (1-3). The general feature – independently also from the value of δ – is that $\langle H_0 \rangle$ does not increase monotonically, there are oscillations mainly at the laser carrier frequency. This corresponds to the periodic motion of the electronic wave packet closer and further away from the nucleus, as it can be seen in Fig. 2, where $\langle z \rangle$ is plotted. Note that when there is no external field ($t < 0$ or $t > \tau$), the Hamiltonian does not contain time dependent terms ($H(t) = H_0$), and $\langle H_0 \rangle$ becomes constant, which is not the case for $\langle z \rangle$, which oscillates already before the arrival of the laser pulse and, in general, still oscillates when the pulse induced external disturbance is over.

The ionization probability P_i also becomes constant for $t > \tau$. By inspecting Fig. 3, we can immediately see that the final ionization probabilities ($P_i(\infty) = P_i(t)$ for $t > \tau$) can be well approximated by oscillating functions of the form

$$I(\delta) = A \sin(\delta + \delta_I) + B. \quad (14)$$

Fitting the actual data, we get $A_{23} = 0.130$, $B_{23} = 0.110$, $A_{34} = 0.010$, $B_{34} = 0.185$ and $A_{45} = 0.010$, $B_{45} = 0.150$ for panels a), b) and c), respectively. These parameters show that the final ionization probability exhibits the strongest δ dependence in the case of Fig. 3 a). In other words, the dynamics of the states (1) are extremely sensitive to the initial phase. This phenomenon can be understood by recalling that for the $2s - 3p$ initial states the carrier frequency ω of the incoming laser field is close to the Bohr frequency of the transition between the states composing the superposition (the transition wavelength is 656.3 nm). The wavelengths of other transitions are more detuned (for $3s$ and $4p$ it is 1875 nm and for $4s$ and $5p$ it is 4051 nm), resulting in weaker δ dependence. (We shall return to the analysis of the average value around which the final ionization probability oscillates in the next subsection.) The relation of the Bohr frequencies and the carrier frequency of the external field can be seen also in Fig. 2, where the most pronounced oscillations are related to $\omega_{nn'}$, while the perturbations change with ω , i.e., the central frequency of the laser pulse. As we can see, the period of the two types of oscillations are the closest for the $2s - 3p$ initial superposition.

The effects shown in Figs. 1-3 can be explained in a simplified, but very intuitive manner: Without external disturbance, the z component of the dipole moment would oscillate with the appropriate Bohr frequency, $\omega_{nn'}$. A weak, almost resonant external field pumps energy into the system and increases the amplitude of the oscillations. However, when the external field is a short pulse containing a few optical cycles only, the relative phase of the free dipole oscillations and that of the excitation is important: the external field can both increase and decrease the amplitude of the dipole oscillations. Clearly, for pulses that can

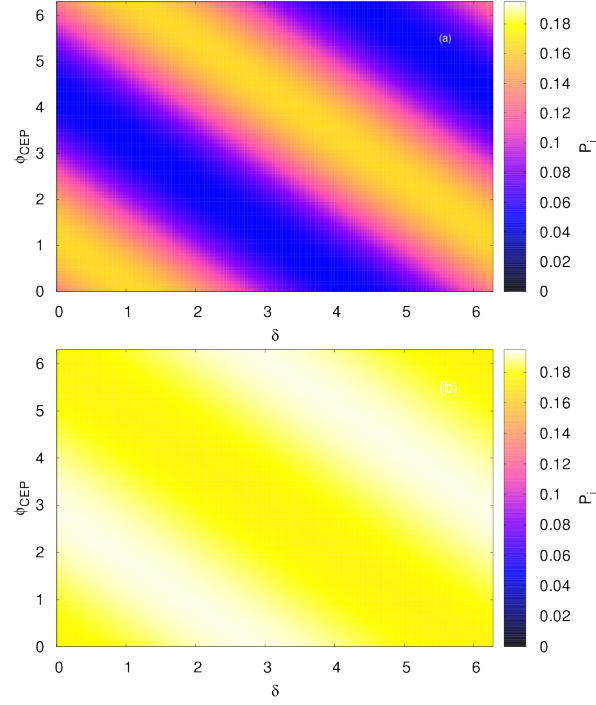


Figure 4. The CEP and the initial phase (δ) dependence of the final ionization probabilities for the initial states (a) ψ_{23} and (b) ψ_{34} (equal weight superpositions). The parameters of the exciting pulse are the same as in Fig. 1.

induce photoionization, strong nonlinear effects appear, numerous states can get excited besides the initial one, etc., so the simple reasoning above can only be relevant around the beginning of the pulse. However, this intuitive picture as an initial approximation points out the role of the interplay between internal, atomic dynamics and the excitation.

More details of this interplay can be investigated by changing the CEP of the exciting pulse as well (which is possible also in an experimental realization). The results are shown in Fig. 4, where the final ionization probabilities are compared for the initial states ψ_{23} and ψ_{34} as a function of δ and ϕ_{CEP} . Here we can also see that for the nearly resonant case (ψ_{23}), considerably more pronounced oscillatory behaviour occurs. More concretely, $P_i(t = \infty, \delta, \phi_{\text{CEP}})$ can again be fitted by sinusoidal functions, in a way that their argument is $\delta + \phi_{\text{CEP}}$. The amplitude of the oscillations is more than ten times larger for the initial states ψ_{23} than for ψ_{34} .

Since although few-cycle sources are available for experimental purposes, but the shorter a pulse is, the more challenging its production is, it is worth investigating whether the phase dependence of the problem is visible for pulses longer than the one we considered so far. To this end, we performed calculations for five longer pulses (6.6–22 fs FWHM in the intensity) with the same peak intensity. The results are shown in Fig. 6. Obviously, longer pulses with the same peak intensity can pump more energy into the atomic system, resulting in higher final ionization probabilities. More interestingly, as we can see, the CEP dependence is still visible (and with current experimental tools it should be also measurable) even for pulses as long as 22 fs consisting of 8 optical cycles, which is a remarkable feature, since for typical strong-field interactions, CEP effects disappear for pulses longer than 2–3 optical cycles. Carrier-envelope phase effects for multi-cycle pulses have only been observed by involving complex extreme ultraviolet spectroscopic techniques in high harmonic generation^{35,36}. Additionally, besides the fundamental perspectives, this feature increases the number of laboratories where our predictions can be tested experimentally.

Superpositions of stationary states with different weights

According to the previous subsection, the relative phase δ between the constituents of the initial superposition, as well as the CEP of the laser pulse can strongly modulate the ionization yield. However, the mean ionization probability, around which oscillations appear as function of δ (or the CEP) has not been analysed so far. As a guideline, it is reasonable to assume that the mean ionization probability mentioned above is determined by the structure of the energy levels. On the other hand, recalling Fig. 3, we see the failure of the naive idea that the closer the expectation value of H_0 to the limit of the continuum (zero level of the energy) in a given initial state, the higher the ionization yield is. (The mean ionization probability is five percent higher for ψ_{34} than for ψ_{45}). By inspecting the level scheme again, we see that the states with principal quantum number $n = 3$ are

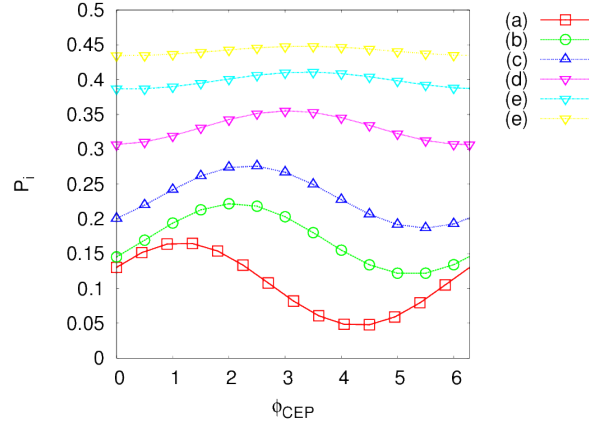


Figure 5. The CEP dependence of the final ionization probability for $\tau = 500, 750, 1000, 1500, 2000$ and 2500 atomic units [(a), (b), ... (f)]. (The corresponding intensity FWHM values are 4.4, 6.6, 8.8, 13.2, 17.6, 22.0 fs, respectively.) The initial state is ψ_{23} with $c_{2s} = c_{3p} = 1/\sqrt{2}$. Additional parameters: 800nm central wavelength, and $E_0 = 2.5$ GV/m.

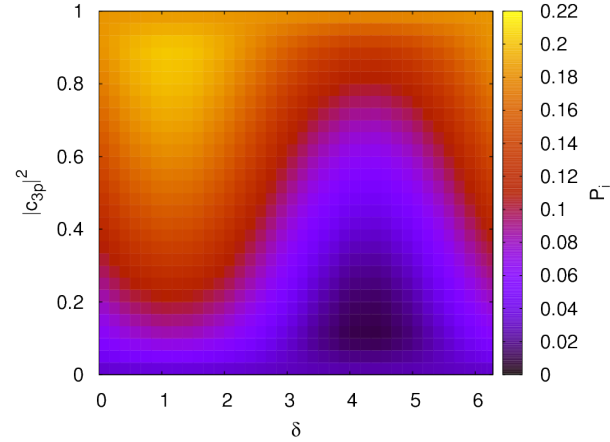


Figure 6. The final ionization probability for the state ψ_{23} as a function of the weight of the state ϕ_{3p} in the superposition and the relative phase δ .

almost resonant with the limit of the continuum (the corresponding wavelength is $9/R_\infty \approx 820$ nm.) Let us recall^{37,38} that for ionization from a stationary state with energy ϵ_n the positions of the ATI peaks can be given by $E_m = m\hbar\omega - U_p - |\epsilon_n|$, where the ponderomotive energy U_p is practically negligible at the laser intensity we considered. That is, the first, strongest ATI peak (corresponding to $m = 1$) is practically at the limit of the continuum for $n = 3$, thus the ionization probability is exceptionally high when the atomic system can be characterized initially by the principal quantum number $n = 3$. As it is shown by Fig. 3, this increased ionization probability is visible even for a superposition when one of the states corresponds to $n = 3$. In order to see how atomic coherence phenomena superimpose on this effect, in Fig. 6 we plotted the final ionization probability of the initial state ψ_{23} as a function of both δ and the weight of the state ϕ_{3p} , i.e., $|c_{3p}|^2$. If the process was completely incoherent the final ionization probability would linearly interpolate between its values valid for the stationary states ϕ_{2s} (corresponding to $c_{3p} = 0$) and ϕ_{3p} (when $c_{3p} = 1$). The oscillations as a function of δ are clear signatures of effects related to the atomic coherence.

Possible experimental realization

The results of the previous sections were obtained by assuming idealized circumstances, without assessing experimental possibilities for the realization of the scheme. Let us now take this aspect into account.

The method we propose is the following: The atomic gas, which is initially in its ground state, is excited by a relatively weak, picosecond pulse (or sequence of pulses) that prepares the superpositions given by Eqs. (1)-(3). Subsequently these states

are probed by the ionizing few-cycle femtosecond pulse. The relative phase δ between the constituents of the superpositions (1)–(3) at the onset of the fs pulse can be – in principle – controlled by appropriately choosing the delay between the preparing pulse and the fs one. In order to obtain the δ dependence of the ionization probability (see Fig. 3), several experimental runs are required, with different time delays between the pulses. The natural time scale on which δ changes is given by the inverse of the Bohr frequencies ω_{nm} [see Eq. (4)], thus the delay between the preparing and the probe pulse should be controlled with a subfemtosecond precision. Additionally, the preparation process has to be robust enough to produce superpositions with stable phase δ . The first (delay) requirement can obviously be satisfied, pump-probe experiments with attosecond delay accuracy can be performed routinely³¹.

Let us now focus on the constancy of δ during a single experimental run. First of all, we should consider a Doppler-free setup, to avoid inhomogeneous broadening. Even in this case, one might think that since different atoms unavoidably have different initial phases (i.e., initially we have $|1s\rangle \exp(i\theta)$, with θ being uniformly distributed between zero and 2π), the value of δ will also have a wide distribution. However, due to the linearity of quantum mechanics, the phase term $\exp(i\theta)$ will be a multiplicative factor during the whole process, i.e., it means a global phase that plays no role in the measurement of physical observables. Similarly, phenomena that ruin quantum mechanical coherence can also be neglected, since their time scale (which is essentially the same as the lifetime of the excited levels) is much longer than the duration of a single experimental run.

The issue which is still to be investigated is if the preparation procedure itself affects the reproducibility of a stable phase difference δ . Since the preparation is a long process, its full quantum mechanical treatment (using the same numerically exact methods that we applied for the ionization process) is computationally prohibitively expensive. However, due to its low intensity, only a few atomic levels play non-negligible role, thus a much simpler calculation that uses the expansion of the wave function on a few energy eigenstates is sufficient. More precisely, a multilevel model including a pair of resonant states can be reliably used to determine the experimental requirements we are interested in. Using a 500-cycle pulse with peak electric field strength having the order of magnitude of MV/m, our simple model-calculations (without the rotating wave approximation) reproduce the predictions of the area theorem²⁷ almost exactly. [That is, the coefficients c in Eqs. (1)–(3) can be controlled precisely by changing either the peak intensity or the duration of the pulse.] Additionally, in complete accordance with textbook results, no additional phase (apart from the one that oscillates with the Bohr frequency) is gained during the preparation process – at exact resonance. This means that a few percent change of the peak intensity or the duration of the preparing pulse induces a few percent change in the coefficients c , but does not affect the relative phase δ . On the contrary, if the carrier frequency ν of the preparing pulse is not exactly the same in the consecutive pulses, δ will also have a distribution with nonzero width. According to our calculations, if one wants to keep the uncertainty of δ below 0.1 rad, the relative deviation $\Delta\nu/\nu$ should be kept below 10^{-5} . This experimental requirement is easily fulfilled. Note that averaging δ over the realistic interval of 0.2 rad results in a less than 5% relative decrease in the amplitude of the oscillations in Fig. 3. Additionally, effects that are related to the population of the energy levels (and not to their coherence) should be detectable even when δ is completely random. Particularly, the mean ionization probabilities that correspond to the different curves in Fig. 3 do not change when δ becomes random.

In summary, the analysis above shows that the experimental techniques that are required to verify our theoretical findings are already available.

Conclusions

We studied the interaction of a hydrogen-like atom in different superposition states and a few-cycle, near infrared laser pulse. The initial atomic states were assumed to be a superposition of s and p states, with different principal quantum numbers. The ionization probability was calculated, and it was found to depend on both the complex amplitude of the constituents of the superpositions and the waveform of the laser pulse. This effect is the strongest when the carrier frequency of the exciting pulse is nearly resonant with the Bohr frequency corresponding to the initial superposition. The origin of this effect – in a simplified, but intuitive picture – is that the “swing” of the internal dipole oscillations can be excited both constructively and destructively, depending on the relative phase of the internal, atomic oscillations and the laser field. For more detuned excitations, this effect was shown to disappear. Furthermore, we found that $2s - 3p$ superposition states enable measurable CEP dependence in the final ionization probability even for pulses as long as 22 fs, corresponding to 8 optical cycles. This is not the case for energy eigenstates, representing a substantial difference between these two initial conditions.

References

1. Krausz, F., Brabec, T., Schnürer, M. & Spielmann, C. *Opt. Photonics News* **9**, 46 (1998).
2. Roudnev, V. & Esry, B. D. General theory of carrier-envelope phase effects. *Phys. Rev. Lett.* **99**, 220406 (2007).
3. de Bohan, A., Antoine, P., Milošević, D. B. & Piraux, B. Phase-dependent harmonic emission with ultrashort laser pulses. *Phys. Rev. Lett.* **81**, 1837–1840 (1998).

4. Baltuska, A. *et al.* Attosecond control of electronic processes by intense light fields. *Nature* **421**, 611–615 (2003).
5. Nisoli, M. *et al.* Effects of carrier-envelope phase differences of few-optical-cycle light pulses in single-shot high-order-harmonic spectra. *Phys. Rev. Lett.* **91**, 213905 (2003).
6. Paulus, G. G. *et al.* Measurement of the phase of few-cycle laser pulses. *Phys. Rev. Lett.* **91**, 253004 (2003).
7. Paulus, G. G. *et al.* Absolute-phase phenomena in photoionization with few-cycle laser pulses. *Nature* **414**, 182–184 (2001).
8. Eremina, E. *et al.* Influence of molecular structure on double ionization of N_2 and O_2 by high intensity ultrashort laser pulses. *Phys. Rev. Lett.* **92**, 173001 (2004).
9. Apolonski, A. *et al.* Observation of light-phase-sensitive photoemission from a metal. *Phys. Rev. Lett.* **92**, 073902 (2004).
10. Dombi, P. *et al.* Direct measurement and analysis of the carrier-envelope phase in light pulses approaching the single-cycle regime. *New Journal of Physics* **6**, 39 (2004).
11. Li, Q., Tong, X.-M., Morishita, T., Wei, H. & Lin, C. D. Fine structures in the intensity dependence of excitation and ionization probabilities of hydrogen atoms in intense 800-nm laser pulses. *Phys. Rev. A* **89**, 023421 (2014).
12. Nakajima, T. Above-threshold ionization by chirped laser pulses. *Phys. Rev. A* **75**, 053409 (2007).
13. Hu, P., Niu, Y., Xiang, Y. & Gong, S. Above-threshold ionization by few-cycle phase jump pulses. *Opt. Express* **21**, 24309–24317 (2013).
14. Scully, M. O. & Zubairy, S. chap. 7 (Cambridge University Press, 1997).
15. Averbukh, V. High-order harmonic generation by excited helium: The atomic polarization effect. *Phys. Rev. A* **69**, 043406 (2004).
16. Gauthey, F. I., Keitel, C. H., Knight, P. L. & Maquet, A. Role of initial coherence in the generation of harmonics and sidebands from a strongly driven two-level atom. *Phys. Rev. A* **52**, 525–540 (1995).
17. Watson, J. B., Sanpera, A., Chen, X. & Burnett, K. Harmonic generation from a coherent superposition of states. *Phys. Rev. A* **53**, R1962–R1965 (1996).
18. Fedorov, M. V. & Movsesian, A. M. Field-induced effects of narrowing of photoelectron spectra and stabilisation of rydberg atoms. *J. Phys B: At. Mol. Opt. Phys.* **21**, L155–L158 (1988).
19. Pont, M. & Gavrilu, M. Stabilization of atomic hydrogen in superintense, high-frequency laser fields of circular polarization. *Phys. Rev. Lett.* **65**, 2362–2365 (1990).
20. Fedorov, M. V. *Atomic and Free Electrons in a Strong Light Field* (World Scientific, Singapore, 1997).
21. Popov, A. M., Tikhonova, O. V. & Volkova, E. A. Field-induced effects of narrowing of photoelectron spectra and stabilisation of rydberg atoms. *J. Phys B: At. Mol. Opt. Phys.* **36**, R125–R165 (2003).
22. Krause, J. L., Schafer, K. J. & Kulander, K. C. Calculation of photoemission from atoms subject to intense laser fields. *Phys. Rev. A* **45**, 4998–5010 (1992).
23. Muller, H. G. An efficient propagation scheme for the time-dependent schrodinger equation in the velocity gauge. *Laser Physics* **9**, 138 – 148 (1999).
24. Nisoli, M., De Silvestri, S. & Svelto, O. Generation of high energy 10 fs pulses by a new pulse compression technique. *Appl. Phys. Lett.* **68**, 2793–2795 (1996).
25. Cavalieri, A. L. *et al.* Intense 1.5-cycle near infrared laser waveforms and their use for the generation of ultra-broadband soft-x-ray harmonic continua. *New Journal of Physics* **9**, 242 (2007).
26. Dombi, P. *et al.* Pulse compression with time-domain optimized chirped mirrors. *Opt. Express* **13**, 10888–10894 (2005). And references therein.
27. Allen, L. & Eberly, J. H. *Optical resonance and two-level atoms* (Wiley, N.Y., 1975).
28. Yatsenko, L. P., Romanenko, V. I., Shore, B. W., Halfmann, T. & Bergmann, K. Two-photon excitation of the metastable $2s$ state of hydrogen assisted by laser-induced stark shifts and continuum structure. *Phys. Rev. A* **71**, 033418 (2005).
29. Jitrik, C. F., Oliverio, Bunge. Transition probabilities for hydrogen-like atoms. *J. Phys. Chem. Ref. Data* **33**, 1059–1070 (2004).
30. Chelkowski, S., Bandrauk, A. D. & Apolonski, A. Phase-dependent asymmetries in strong-field photoionization by few-cycle laser pulses. *Phys. Rev. A* **70**, 013815 (2004).

31. Krausz, F. & Ivanov, M. Attosecond physics. *Rev. Mod. Phys.* **81**, 163–234 (2009).
32. Bandrauk, A. D., Fillion-Gourdeau, F. & Lorin, E. Atoms and molecules in intense laser fields: gauge invariance of theory and models. *J. Phys. B: At. Mol. Opt. Phys.* **46**, 153001 (2013).
33. Reiss, H. R. The tunnelling model of laser-induced ionization and its failure at low frequencies. *J. Phys. B: At. Mol. Opt. Phys.* **47**, 204006 (2014).
34. Peaceman, D. W. & Rachford, H. H. The numerical solution of parabolic and elliptic differential equations. *Journal of the Society for Industrial and Applied Mathematics* **3**, 28 – 41 (1955).
35. Sansone, G. *et al.* Observation of carrier-envelope phase phenomena in the multi-optical-cycle regime. *Phys. Rev. Lett.* **92**, 113904 (2004).
36. Tzallas, P., Skantzakis, E. & Charalambidis, D. Measuring the absolute carrier-envelope phase of many-cycle laser fields. *Phys. Rev. A* **82**, 061401 (2010).
37. Faisal, F. H. M. & Scanzano, P. *Phys. Rev. Lett.* **68**, 2909 (1992).
38. Kopold, R., Becker, W., Kleber, M. & Paulus, G. G. Channel closing effects in high order att and hhg. *J. Phys. B: At. Mol. Opt. Phys.* **35**, 217–232 (2002).

Acknowledgements (not compulsory)

We acknowledge support from the Hungarian Academy of Sciences (“Lendület” Grant). This work was also partially supported by the European Union and the European Social Fund through project entitled “ELI Team at the University of Szeged”, and by the National R&D Office of Hungary under contracts No. 81364 and 109257.

Author contributions statement

V.A. performed the theoretical formulation, numerical simulation and the data collection. M.G.B. initiated the concept of the manuscript. V.A. and F.P. conducted the numerical simulations. V.A. prepared the figures. V.A., M.G.B., P.D. and P.F. analysed the results. V.A. and P.F. wrote the main manuscript text. All authors reviewed the manuscript.

Additional information

Competing financial interests

The authors declare no competing financial interests.